AN EXPERIMENTAL STUDY ON AIR-WATER COUNTERCURRENT FLOW LIMITATION IN THE UPPER PLENUM WITH A MULTI-HOLE PLATE

HEE CHEON NO*, KYUNG-WON LEE and CHUL-HWA SONG[1]
Korea Advanced Institute of Science and Technology
373-1 Guseong-dong, Yuseong-gu, Daejeon 305-701, Korea
[1]Korea Atomic Energy Research Institute
150 Dukjin-dong, Yuseong-gu, Daejeon 305-353, Korea
*Corresponding author. E-mail : hcno@kaist.ac.kr

Received October 25, 2005

Air-water countercurrent flow limitation at perforated plates with four holes was investigated in a vertical tank to see the effects of the plate thickness, the number of hole, and the diameter of the hole on the onset of CCFL. The thickness of plates was 1 cm and 4 cm, with a relatively large hole diameter of 5 cm. The collapsed water level formed on the perforated plate and its distribution in the upper plenum were measured. The gas flow rate in the multi-hole plate is relatively higher than one in the single tube because some of holes in the multi-hole plate provide a flow path for liquid with less air-liquid resistance than in the single tube. The onset of CCFL occurred at nearly the same air flow rate regardless of the plate thickness. The negligible effect of the plate thickness on CCFL means that the flooding is initiated at the top of the plate rather than at its bottom. It turns out that j_k^* and K_k better fit the data than H_k^* when hole diameter is greater than 2.86 cm. In our experimental ranges, the collapsed water levels at the onset of CCFL ranged from 7.5 cm to 10.5 cm. There was no three dimensional distribution of water level before and after the onset of CCFL.

KEYWORDS : CCFL, Flooding, Multiple Holes, Perforated Plate, Upper Plenum

1. INTRODUCTION

Countercurrent flow limitation (CCFL), or flooding, at the upper core support plate (UCSP) or tie plate is one of the most important phenomena in the safety of a pressurized water reactor (PWR). During a reflood phase of large break loss of coolant accident (LBLOCA), steam-water countercurrent flow occurs between the steam flow from the core region and the water de-entrained in the upper plenum. At sufficiently high steam flow, however, countercurrent flow of steam and water can be limited at the UCSP or tie plate due to the small flow area, which results in water accumulation in the form of a two-phase mixture pool in the upper plenum (Damerell and Simons, 1993).

The water de-entrained in the upper plenum supplies additional cooling water, improving core cooling. Accordingly, water accumulation by CCFL reduces the effectiveness of core cooling and delays the core flooding rate by creating a static head pressure drop. Some PWRs inject partial emergency core cooling water directly to the upper plenum or into the hot-legs. In these cases, CCFL prevents cooling water from penetrating into the core. Therefore, it is very important to investigate the factors affecting the onset of CCFL at the UCSP or tie-plate.

Over the past five decades, various parametric effects of flow conditions and tube geometries on CCFL phenomena have been investigated for a single tube (Wallis [2], Bankoff and Lee [3]). The CCFL mechanisms at short multi-hole plates are much more complicated than those in single vertical tube due to the interaction between neighboring holes and global oscillation of the two-phase liquid pool formed above the multi-hole plates.

The effects of the short multiple flow paths and flow conditions on CCFL phenomena have been evaluated. Bankoff et al. [4] studied the liquid downwards penetration of a bubbly water pool above a perforated plate. They developed empirical correlations with and without condensation to predict the liquid penetration rate using a new scaling parameter (H^*), which interpolates between the dimensionless superficial velocity (j^*) and the Kutateladze number (K). Lee et al. [5] investigated the effects of geometric and flow factors on CCFL in test section with a multi-hole plate. The gas flow required for the onset of

CCFL was greater for the larger number of flow paths. The liquid carry-over for fixed gas flow rate was much smaller for the larger number of paths due to the comparatively weak interaction between gas and liquid. Sobajima [6] found that CCFL correlations strongly depended on the hole size, hole-end geometry and plate thickness. Observations for the range of partial liquid penetration showed that some holes were fully occupied by liquid down flow, while the other holes were governed by upward gas flow. The location of the liquid-filled holes was random.

Celata et al. [7] examined the effect of orifice-type flow obstructions on CCFL in a vertical tube. Their experimental results for a plate with the same flow area but with different number of holes showed that the behavior of the onset of CCFL and liquid zero penetration was similar; a systematically greater liquid entrainment occurred in the single-hole plate due to the ticker liquid film with respect to the multi-hole plate. According to the experimental results, Kokkonen and Tuomisto [8] found that the liquid head above the perforated plate has a minor, but clearly distinct, effect on the CCFL curve. At very low air flow rate, the volume below the perforated plate and the plate thickness affected CCFL behavior. The diameter of flow channel also affected the CCFL behavior. Zhang et al. [9] investigated the hydrodynamic mechanisms relevant to CCFL phenomenon in air-water countercurrent flow through short multi-tube geometries. They reported two kinds of hydrodynamic instabilities, local interfacial instability and global flow instability, which were responsible for CCFL. They showed that a shorter tube length might enhance liquid penetration.

Test section geometries and objectives of previous studies are summarized in Table 1. CCFL data for a perforated plate were strongly dependent on the plate geometry, including hole diameter, numbers of holes and entry geometry [4-9]. There is no experimental data applicable to plates with large hole diameter like the UCSP. Here, we investigated air-water countercurrent flow limitation at perforated plates with relatively large hole diameter in a vertical tank to see the effect of the plate thickness, the number of hole, and the diameter of the hole on the onset of CCFL.

2. EXPERIMENTAL WORKS

2.1 Experimental Apparatus

The schematic diagram of the experimental apparatus

Table 1. Test Section Geometries and Objectives of Previous Studies

	Test Section Geometries						Main Objectives
	Tube Diameter (cm)	Plate Thickness (cm)	Plate Hole Diameter (cm)	No. of Holes	Pitch (cm)	Perforation Ratio (%)	
Bankoff et al. [4]	7.15 ×4.29 rectangular channel	2	0.48, 1.05, 2.86	2, 3, 5, 9, 15,40	- 3.58 (5 cases)	8.47 - 42.34 (6 cases)	CCFL
Lee et al. [5]	10.08	1.27	2.57 ~ 7.62 (5 cases)	1, 2, 3		19.4 - 57.1 (3 cases)	CCFL, Water carry-over rate
Sobajima [6]	7.64 ×7.64 rectangular channel	1.5, 2	1.05, 2.0	25	1.43	37.1, 48.4	CCFL
Celata et al. [7]	1.62, 2	0.12- 0.2	0.7 ~ 1.9 (9 cases)	1, 4	-	36 - 100 (8 cases)	CCFL
Kokkonen and Tuomisto [8]	6, 14.1, 16.5, 23.4	0.3, 2	0.5 & elongated holes	5 - 889 (5 cases)	-	36, 41, 44	CCFL
Zhang et al. [9]	10	7.2, 36, 72	3.6	3	11.6	38.9	CCFL
Present Experiment	48	1,4	5	4	9.6	4.3	Onset of CCFL

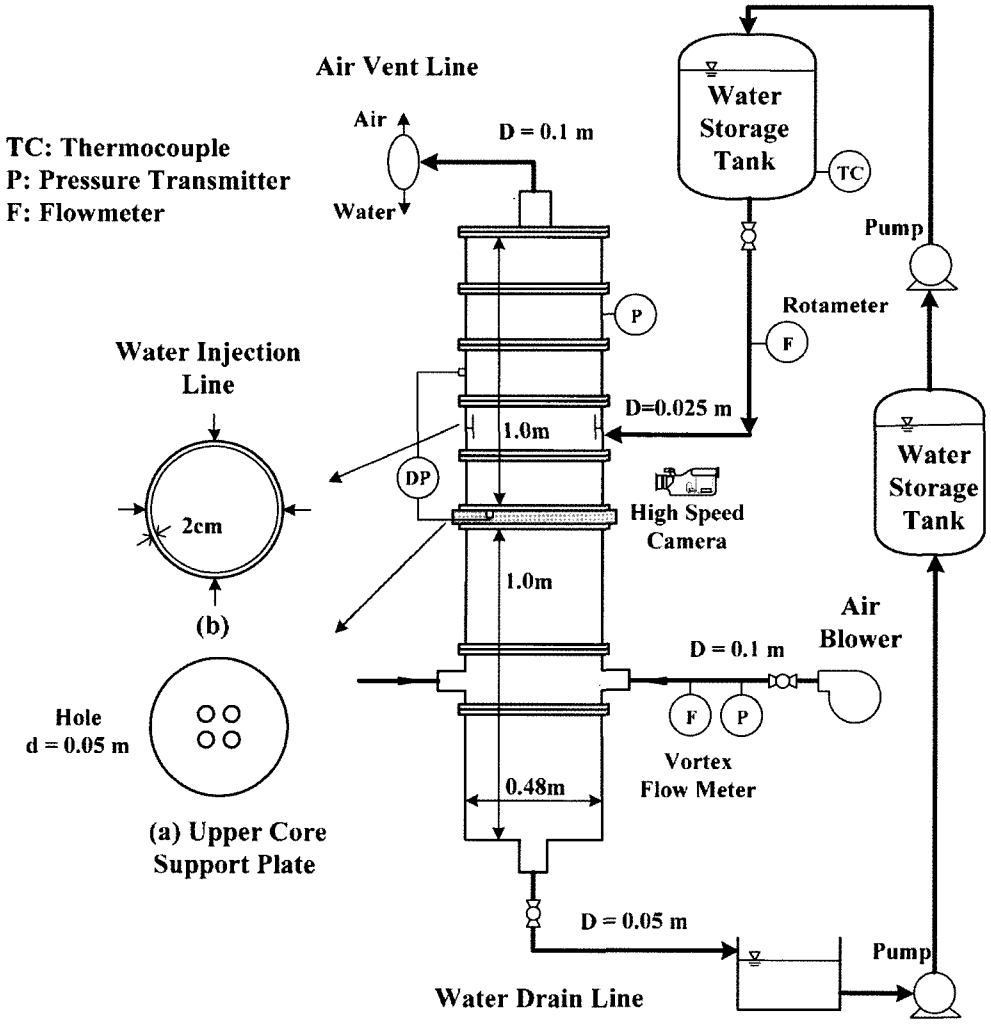

Fig. 1. Schematic Diagram of Experimental Apparatus

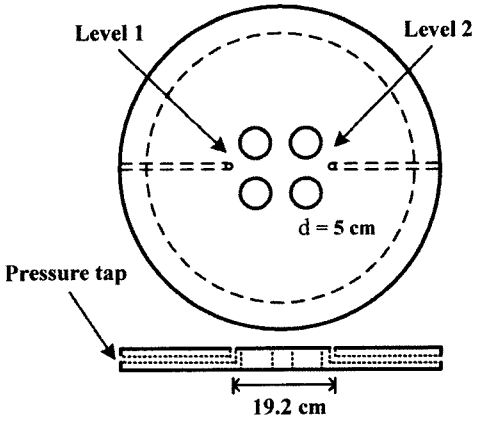

Fig. 2. Plate Geometry

is shown in Figure 1. The main components of the system are test section, water supply, air supply and the data acquisition systems. Flow conditions in the upper plenum during the reflood phase of the LBLOCA were simulated using air and water.

The perforated plate with 4 holes (0.05 m in diameter and 0.096 m in pitch) was installed at the middle height of the vessel (2 m in height and 0.48 m in inner diameter) to simulate the UCSP and the upper plenum of a PWR (Fig. 1(a)). The plates were made of transparent acrylic material (1cm and 4cm thick) with sharp edges (Figure 2). The perforation ratio of plate was 4.3%. Two pressure taps were placed on the plates to measure the collapsed water level on the plates. The distance between two pressure taps was 19.2 cm.

Water was supplied from the water storage tank at a constant head and injected into the upper plenum through four water injection lines. The distance from the water injection lines and the plates was 25 cm. A concentric barrier was installed inside the test vessel (Fig. 1(b)). The injected water in the upper plenum bumps into this barrier, spreads widely, and flows downward. The gap between the vessel and the barrier was 2 cm. Water drained from the test vessel was collected in the drain storage tank and returned by two water pumps to the water storage tank. The water flow rate was measured by four rotameters within an accuracy of $\pm 5\%$.

Air, supplied by a blower, was injected into the lower plenum through two air injection lines, passing through the plate holes, the upper plenum and the air vent line. The air flow rate was measured by a vortex flow meter within an accuracy of $\pm 3\%$.

2.2 Test Parameters and Procedure

Plate thickness was 1 cm and 4 cm. Water flow rate was held constant, while the air flow rate was increased stepwise. The range of water superficial velocities (j_f) at holes was from 0.021 to 0.076. The onset of CCFL was determined by the change in collapsed water level on the plates. The collapsed water level was determined by measuring the change in pressure difference between the bottom and the top of the upper plenum. The experimental procedure consisted of: (a) a given flow rate of water was supplied into the upper plenum, (b) air was supplied into the lower plenum, and (c) after allowing sufficient time to reach a quasi-steady state, air flow rate was increased stepwise until the onset of CCFL was observed. This procedure was repeated for various water flow rate.

2.3. Definition of Onset of CCFL

The relationship between time and air flow and onset of CCFL is shown in Fig. 3. At a very low air flow rate, air and water flowed countercurrently in the form of the separated flow without large disturbances (Region A; Fig. 3). As the air flow rate increased, air-water mixing suddenly occurred in plate holes, and air-water two-phase mixture level began to increase dramatically. This point is defined as the onset of water accumulation. Beyond the onset of water accumulation, both the air-water mixture level and the collapsed water level remained constant, increasing with an increase in the air flow rate (Region B; Fig. 3). This means that the entire water injected into the upper plenum flowed completely downward. As a result, there was no real limitation of downward water flow. As the air flow rate was further increased, there came a point at which the collapsed water level increased continuously even at a constant air flow rate (Region C; Fig. 3). In this region, the water penetration rate through the plate is smaller than the injected water flow rate (partial liquid penetration). In this study, this point is defined as the onset of CCFL.

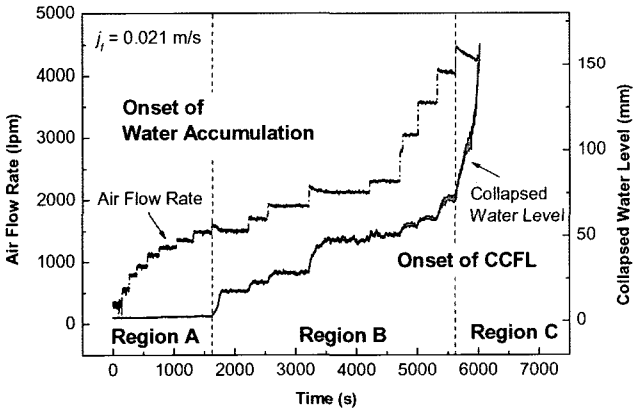

Fig. 3. Onset of Water Accumulation and CCFL

Lee et al. (1982) defined the onset of CCFL as the occurrence of significance liquid carry-over (at least 2% of the liquid injection rate) or a sudden increase in pressure drop across the plate. Celata et al. (1989) defined the onset of CCFL as the point at which the liquid falling film begins to be entrained by the upward-flowing gas. Zhang et al. (1992) defined the onset of CCFL as the point the penetration velocity begins to decrease, which is the same as our definition. These phenomena occur simultaneously.

3. CCFL CRITERIA

The most widely used flooding (or CCFL) correlations are Wallis type [2,4,6,7,9] and Kutatetladze type [4,5,6,8,9] correlations, expressed as:

$$j_g^{*\,1/2} + m_w j_f^{*\,1/2} = C_w, \tag{1}$$

$$K_g^{\,1/2} + m_k K_f^{\,1/2} = C_k, \tag{2}$$

where m and C are empirically determined constants. The parameters, j_k^* and K_k, are the dimensionless superficial velocity and the Kutateladze number of each phase k (f denotes liquid phase and g denotes gas phase), respectively, expressed as:

$$j_k^* = j_k \left[\frac{\rho_k}{g d(\rho_f - \rho_g)} \right]^{1/2}, \tag{3}$$

$$K_k = j_k \left[\frac{\rho_k^{\,2}}{g\sigma(\rho_f - \rho_g)} \right]^{1/4}. \tag{4}$$

In the above equations, j_k and ρ_k are the superficial velocity and the density of each phase of k, and d and σ are the hole diameter and the surface tension respectively.

For perforated plates, Bankoff et al. [4] suggested a correlation using the dimensionless parameter H_k^*, expressed as:

$$H_g^{*\,1/2} + H_f^{*\,1/2} = C_b, \tag{5}$$

where H_k^* is the dimensionless flux of each phase of k and has the form:

$$H_k^* = j_k \left[\frac{\rho_k}{g w (\rho_f - \rho_g)} \right]^{1/2}, \tag{6}$$

where w is the interpolative length scale given by:

$$w = d^{1-\beta} L_l^{\beta} \quad (0 \le \beta \le 1), \tag{7}$$

$$L_l = \left[\frac{\sigma}{g(\rho_f - \rho_g)} \right]^{1/2}, \tag{8}$$

$$\beta = \tanh(\gamma k_c d), \tag{9}$$

$$k_c = 2\pi / t_p, \tag{10}$$

where L_l is the Laplace capillary constant, k_c is the critical wave number and t_p is the plate thickness. The parameter γ is the perforation ratio, defined as the ratio of the total area of holes to the flow area of tank.

Equations 6 through 10 imply that the parameter H_k^* approaches j_k^* for small hole diameters, small perforation ratios, and large plate thickness, while it approaches K_k for large hole diameters, large perforation ratios and thin plates.

The parameter C is a function only of geometry and reflects entrance and exit effects, Bankoff et al. [4] suggested C of the form:

$$\begin{aligned} C_b &= 1.07 + 4.33 \times 10^{-3} L^* \quad (L^* < 200), \\ C_b &= 2 \qquad\qquad\qquad\quad (L^* > 200), \end{aligned} \tag{11}$$

where L^* is a Bond number defined as

$$L^* = n\pi d \left[\frac{g(\rho_f - \rho_g)}{\sigma} \right]^{1/2} \tag{12}$$

and n is the number of holes and g is the acceleration of gravity.

4. RESULTS AND DISCUSSION

4.1 Effects of the Water Flow Rates and the Plate Thickness on the Onset of CCFL

Our experimental data for the onset of CCFL are shown in Figs. 4-6. The characters d, t, n, and p refer to the hole diameter, the plate thickness, the number of holes, and the pitch between neighboring holes, respectively. The CCFL data for the plate thickness of 1 cm and 4 cm were plotted in the form of dimensionless superficial velocities (j_k^*), the Kutateladze number (K_k), and the interpolation scaling parameter (H_k^*) based on the flow area of plate holes. The parameters, j_k^*, K_k and H_k^* were calculated from the water flow rate injected into the upper plenum since there was no difference between the injected water flow rate and the

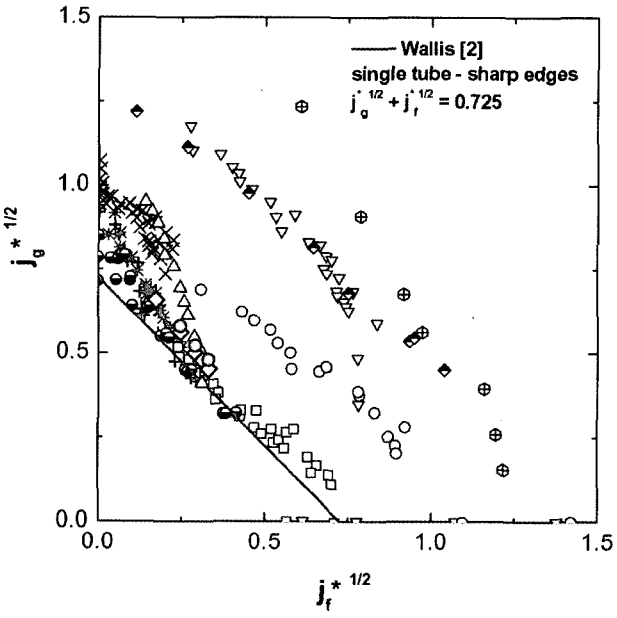

Fig. 4. CCFL Data in j^* Scaling

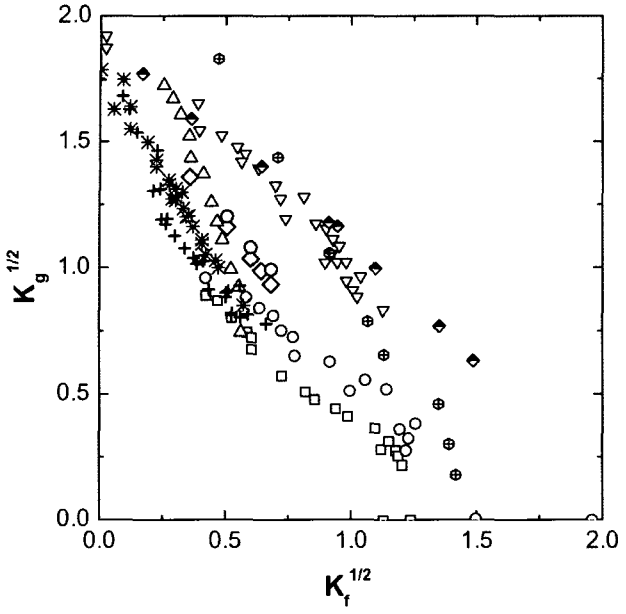

		d(cm)-t(cm) - n - p(cm)
○	Present Data	5 - 1 - 4 - 9.6
◇	Present Data	5 - 4 - 4 - 9.6
□	Bankoff [4]	2.86 - 2 - 2 - 3.58
○	Bankoff [4]	1.05 - 2 - 3 - 1.43
▽	Bankoff [4]	1.05 - 2 - 15 - 1.43
△	Lee [5]	2.93 -1.27 - 3
◆	Sobajima [6]	1.05 - 2 - 25 - 1.43
⊕	Kokkonen [8]	0.5 - 2 - 52
✳	Zhang [9]	3.6 - 7.2 - 3 - 11.6
+	Zhang [9]	3.6 - 72 - 3 - 11.6

Fig. 5. CCFL Data in K Scaling

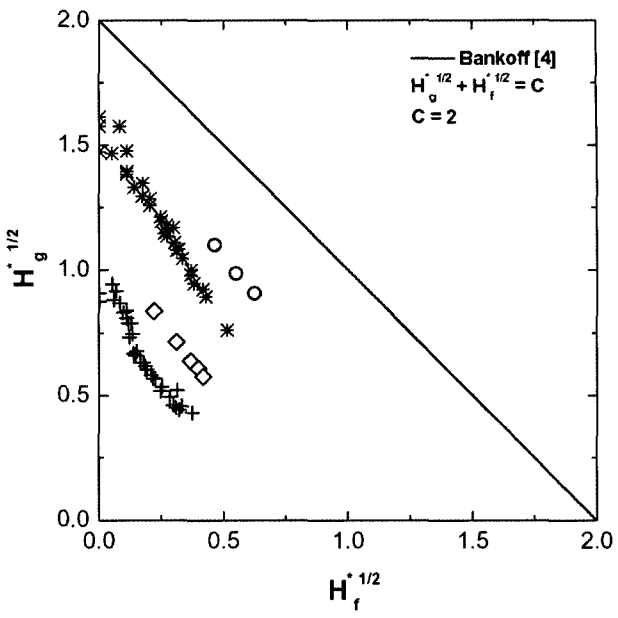

		d(cm)-t(cm)-n-p(cm)
○	Present Data	5 - 1 - 4 - 9.6
◇	Present Data	5 - 4 - 4 - 9.6
✳	Zhang [9]	3.6 - 7.2 - 3 - 11.6
+	Zhang [9]	3.6 - 72 - 3 - 11.6

Fig. 6. CCFL Data in H^* Scaling

downward penetration flow rate through the plate before the onset of CCFL.

The air flow rate per hole required for the onset of CCFL decreased as the water flow rate increased due to the formation of thick water films that promote interfacial instability. The onset of CCFL occurred at nearly the same air flow rate regardless of plate thicknesses. The negligible effect of the plate thickness on CCFL means that the flooding is initiated at the top of the plate rather than at its bottom. The results of Sobajima [6] and Jeong and No [10] also showed that the length effect on CCFL was significant only when the entrance and exit geometry were smooth. Data expressed with j_k^* or K_k scaling, were nearly the same both plate thicknesses (Figs. 4 and 5).

However, data expressed as H_k^* scaling, showed difference between the two plate thicknesses (Figure 6) because the value of H_k^* depends on the plate thickness. The parameter H_k^* approaches j_k^* for thick plate, while it approaches K_k for thin plate.

4.2 Comparison of Present Data with Previous Results

Our experimental data were compared with the data of Wallis [2], Bankoff et al. [4], Lee et al. [5], Sobajima [6], Celata et al. [7], Kokkonen and Tuomisto [8] and Zhang et al. [9]. The air flow rate required the onset of CCFL in the multi-hole plate is relatively higher than one in the single tube because some of holes in the multi-hole plate provide a flow path for liquid with less air-liquid resistance than in the single tube [5].

As shown in Figs. 4 and 5, plotting CCFL data in the form of j_k^* or K_k shows that j_k^* and K_k well fit the data when hole diameter is greater than 2.86 cm. On the other hand, the data with small hole diameters of 0.5 cm and 1.05 cm showed a considerable deviation from other data in the multi-hole plates with larger hole diameters. Our data expressed as j_k^* agreed well with Bankoff et al.'s data for a relatively smaller number of holes (n = 2 and d = 2.86 cm) and Zhang et al.'s data.

Our data expressed as H_k^* were also compared with Bankoff et al.'s and Zhang et al.'s (Fig. 6). There was a large difference between our data and Bankoff et al.'s correlation (Eqs. (5) and (11)) as well as between our data

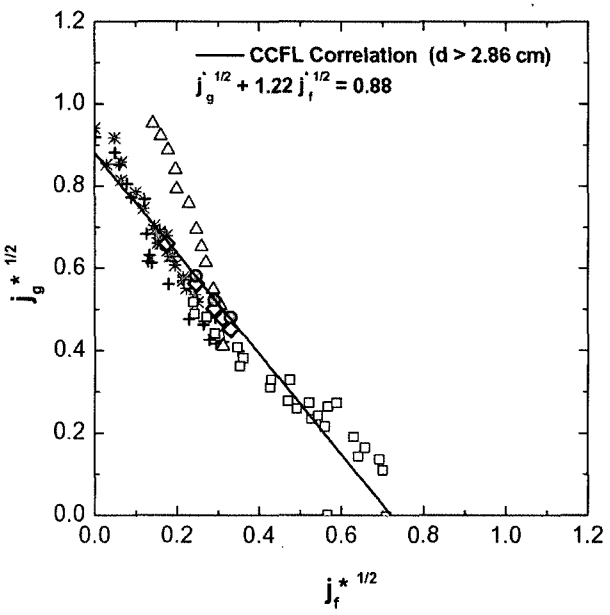

		d(cm)-t(cm) -n - p(cm)
o	Present Data	5 - 1 - 4 - 9.6
◇	Present Data	5 - 4 - 4 - 9.6
□	Bankoff [4]	2.86 - 2 - 2 - 3.58
△	Lee [5]	2.93 - 1.27 - 3
✳	Zhang [9]	3.6 - 7.2 - 3 - 11.6
+	Zhang [9]	3.6 - 72 - 3 - 11.6

Fig. 7. Comparison of Experimental Data with the Developed CCFL Correlation

and Zhang et al.'s. These differences may be due to differences in plate hole diameter, plate thickness and perforation ratio. Our experimental data also showed that the nondimensional parameter H_k^* overestimated the effect of plate thickness.

Based on Figures 4 through 6, it is clear that j_k^* and K_k better fit the data than H_k^* when the hole diameter is greater than 2.86 cm. On the basis of Bankoff et al.'s [4] (d =2.86 cm), Lee et al.'s [5], Zhang et al.'s [9] and our experimental data, we developed a Wallis type correlation with the standard deviation of 0.081 as follows:

$$j_g^{*1/2} + 1.22 j_f^{*1/2} = 0.88 \qquad \text{for } d \geq 2.86 \text{ cm} \qquad (13)$$

The comparison of experimental data with the developed CCFL correlation, Eq. (13), is shown in Fig. 7.

4.3 Collapsed Water Level in the Upper Plenum and Its Distribution

The collapsed water level formed on the perforated plate

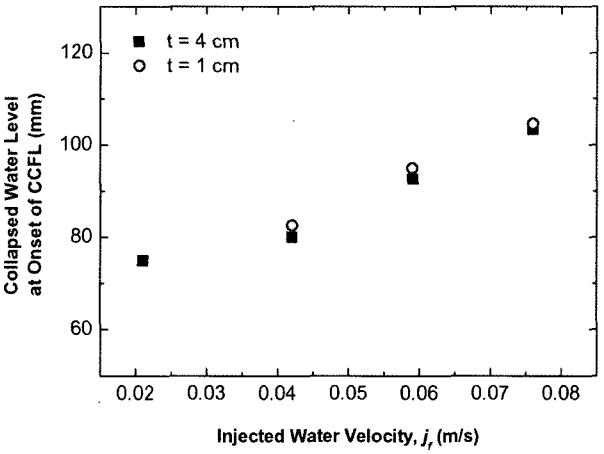

Fig. 8. Collapsed Water Level Formed on the Plate at the Onset of CCFL

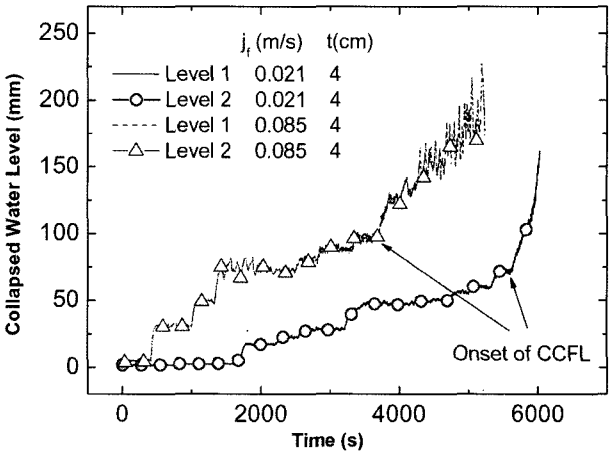

Fig. 9. Distribution of Collapsed Water Level in the Upper Plenum

at the onset of CCFL is shown in Fig. 8. In our experimental ranges, the collapsed water levels at the onset of CCFL ranged from 7.5 cm to 10.5 cm. The results show that the collapsed water level increased as the water flow rate injected into the upper plenum increased. The plate thickness had a negligible effect on the collapsed water level.

The distribution of the collapsed water level in the upper plenum is shown in Fig. 9. The water levels were measured at different two locations, namely, Level 1 and Level 2 in Fig. 2. There was no difference in water levels between the two locations before and after the onset of CCFL, and theses results mean there was no three dimensional distribution of collapsed water level. The collapsed

water levels were highly agitated at relatively high-injected water flow rate.

4.4 Uncertainty Analysis

The measurement errors of flow temperature, water flow rate, and air flow rate were ±2.2°C, ±5%, and ±3%. We analyzed the uncertainties of the dimensionless flow velocities using the error propagation method (Kline and McClintock [11]). The estimated uncertainties of K_f, K_g, H_f^* and H_g^* are ±9.8%, ±5.6%, ±9.8%, and ±5.9% with 95% confidence level.

5. CONCLUSIONS

We investigated air-water CCFL through large hole diameter multi-hole plates and obtained the data for the onset of CCFL. The air flow rate required for the onset of CCFL was independent of the plate thicknesses of 1 cm and 4 cm: the flooding is initiated at the top of the plate rather than at its bottom. The air flow rate required the onset of CCFL in the multi-hole plate is relatively larger than one in the single tube because some of holes in the multi-hole plate provide a flow path for liquid with less air-liquid resistance than in the single tube. It turns out that j_k^* and K_k better fit the data than H_k^* when hole diameter is greater than 2.86 cm. There was no three dimensional distribution of water level before and after the onset of CCFL.

REFERENCES

[1] P. S. Damerell and J. W. Simons, "Reactor Safety Issues Resolved by the 2D/3D Program," NUREG/IA-0127 (1993).

[2] G. B. Wallis, One-dimensional Two-phase Flow, McGraw-Hill, New York, 336-345, 1969.

[3] S. G. Bankoff and S. C. Lee, Multiphase Science and Technology, Vol. 2 (Edited by G.F. Hewitt, J.M. Delhaye, N. Zuber), Chapter 2, A Critical Review of the Flooding Literature, Hemisphere, New York (1985).

[4] S. G. Bankoff, R. S. Tankin, M. C. Yuen and C. L. Hsieh, "Countercurrent Flow of Air/Water and Steam/Water Through a Horizontal Perforated Plate," *Int. J. Heat Mass Transfer*, **24**, 8, 1381-1395 (1981).

[5] H. M. Lee, G. E. McCarthy and C. L. Tien, "Liquid Carry-over and Entrainment in Air-water Countercurrent Flooding," EPRI report, NP-2344 (1982).

[6] M. Sobajima, "Experimental Modeling of Steam-Water Countercurrent Flow Limit for Perforated Plates," *J. Nuclear Science and Technology*, **22**, 9, 723-732 (1985).

[7] G. P. Celata, N. Cumo, G. E. Farello, and T. Setaro, "The Influence of Flow Obstructions on the Flooding Phenomenon in Vertical Channels," *Int. J. Multiphase Flow*, **15**, 2, 227-239 (1989).

[8] I. Kokkonen and H. Tuomisto, "Air/Water Countercurrent Flow Limitation Experiments with Full-Scale Fuel Bundle Structures," *Experimental Thermal and Fluid Science*, **3**, 581-587 (1990).

[9] J. Zhang, J. M. Seynhaeve and M. Giot, "Experiments on the Hydrodynamics of Air-Water Countercurrent Flow Through Vertical Short Multitube Geometries," *Experimental Thermal and Fluid Science*, **5**, 755-769 (1992).

[10] J. H. Jeong and H. C. No, "Experimental Study of the Effect of Pipe Length and Pipe-end Geometry on Flooding," *Int. J. Multiphase Flow*, **22**, 1, 499-514 (1996).

[11] S. J. Kline and F. A. McClintock, "Describing Uncertainties in Single Sample Experiments," *Mechanical Engineering*, **75**, 3-8 (1953).